

Topologically protected Landau levels in bilayer graphene in finite electric fields

Tohru Kawarabayashi,¹ Yasuhiro Hatsugai,^{2,3} and Hideo Aoki⁴

¹*Department of Physics, Toho University, Funabashi, 274-8510 Japan*

²*Institute of Physics, University of Tsukuba, Tsukuba, 305-8571 Japan*

³*Kavli Institute for Theoretical Physics, University of California, Santa Barbara CA 93106, USA*

⁴*Department of Physics, University of Tokyo, Hongo, Tokyo 113-0033 Japan*

(Dated: November 28, 2011)

The zero-energy Landau level of bilayer graphene is shown to be anomalously sharp (delta-function like) against bond disorder as long as the disorder is correlated over a few lattice constants. The robustness of the zero-mode anomaly can be attributed to the preserved chiral symmetry. Unexpectedly, even when we apply a finite potential difference (i.e., an electric field) between the top and the bottom layers, the valley-split $n = 0$ Landau levels remain anomalously sharp although they are now shifted away from the zero energy, while the $n = 1$ Landau levels exhibit the usual behavior.

Introduction — The existence of the zero-energy Landau level is a most fundamental property of the electronic states in graphene in magnetic fields, which hallmarks the unconventional quantum Hall effect observed in monolayer graphene.^{1,2} Specifically, the zero-energy Landau level of mono-layer graphene shows an anomalous robustness against the disorder induced by ripples, an intrinsic disorder in graphene, which leads to an unconventional criticality of Hall transition at zero energy.^{3,4} For the robustness of zero modes, the chiral symmetry,⁵ defined in terms of the chiral operator Γ that anti-commutes with the Hamiltonian H , $\{\Gamma, H\} = 0$ with $\Gamma^2 = 1$, is an essential ingredient.⁶ For monolayer graphene, we have vertical Dirac cones at K and K' points in the Brillouin zone, and the effective Hamiltonian has the chiral symmetry. In such a system, it has been demonstrated by the present authors that the zero-energy ($n = 0$) Landau level is robust against the disorder that respects the chiral symmetry as long as the disorder is correlated over a few lattice constants.^{7,8} Experimentally, the $n = 0$ Landau level narrower than the other $n \neq 0$ Landau levels is reported for monolayer graphene,⁹ which is consistent with the present robustness specific to the zero-energy ($n = 0$) Landau level.

The notion of the chiral symmetry is so universal that it has further been shown¹⁰ that the chiral symmetry, usually considered for the vertical Dirac cones, can be generalized to accommodate tilted Dirac cones, such as those encountered in certain organic metals.^{11–13} The generalized chiral symmetry protects the zero-energy Landau level as far as the Hamiltonian as a differential operator is elliptic, where we can even extend the argument of Aharonov and Casher for counting the number of zero modes in the presence of disorder.¹⁴ The existence of the generalized chiral symmetry can indeed be translated to a condition that the index theorem¹⁵ holds for generic tilted Dirac cones. The chiral symmetry is therefore directly related to the robustness of zero modes for the massless Dirac fermions.

Now, in the physics of graphene, the case of bilayer graphene is an interesting test bench for examining various graphene properties. Specifically, McCann and Falko

have shown that there exist four-fold degenerated (per spin) zero-energy Landau levels, which lead to a quantum Hall effect characteristic to bilayer graphene.¹⁶ The degeneracy comes from the valley (K and K') degrees of freedom and two ($n = 0$ and $n = 1$) Landau indices. Although the robustness of these zero mode Landau levels is also predicted as a consequence of the index theorem,^{17,18} it is not clear whether there is also a direct relationship between the *chiral symmetry* and the anomalous robustness of zero modes, since the parabolic band dispersion in the bilayer graphene, as opposed to the linear one in the monolayer graphene, might well invalidate the arguments. For instance, the robustness of the $n = 0$ level and that of $n = 1$ level can naively be different, since they have different structure for the wave functions.

The difference becomes even greater when we apply an electric field perpendicular to the graphene sheet, which introduces an energy gap. An opening of the energy-gap in bilayer systems is important in an applicational context as well.^{21–23} Thus a further interest is to see what happens to the zero-energy Landau level when the energy gap is introduced. Experimentally, it is desirable to clarify quantitatively the robustness of the zero modes in bilayer graphene, since experimental results in high mobility samples are now available.^{19,20}

The purpose of the present paper is to explore these very questions, for which we have performed numerical studies based on the lattice model. We shall show that both the $n = 0$ and the $n = 1$ Landau levels in bilayer graphene are robust against bond disorders as long as they are correlated over a few lattice constants. We analyse the result in terms of the chiral symmetry for the bilayer system. Unexpectedly, it is further found that, even in the presence of a potential difference (an electric field) between the top and the bottom layers, the $n = 0$ Landau levels remain robust although they are shifted away from zero energy, while the $n = 1$ Landau levels exhibit the usual behavior. This phenomenon is also discussed in terms of the effective theory at K and K' points.

Lattice model — In order to investigate the robustness of the zero modes against disorder in bilayer graphene, we adopt the following tight-binding lattice model with

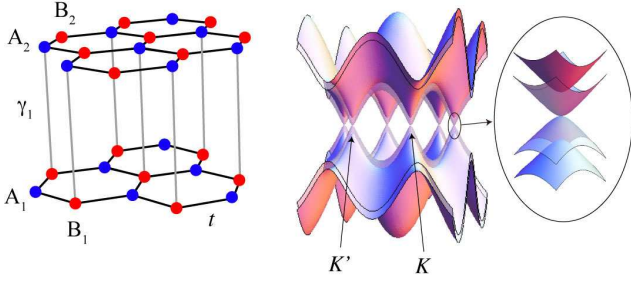


FIG. 1: (Color Online) For a bilayer graphene we show the A-B stacking with the interlayer coupling γ_1 (left panel), and the band dispersions (right). $\mathbf{K} = (2\pi/3\sqrt{3}, 2\pi/3)a^{-1}$ and $\mathbf{K}' = (-2\pi/3\sqrt{3}, 2\pi/3)a^{-1}$ are the corners of the Brillouin zone.

the Bernal (A-B) stacking.¹⁶ We assume that each layer can be described by the simple honeycomb lattice, while the interlayer coupling, γ_1 , connects a site (B_1) on the B sublattice of the bottom layer and a site (A_2) on the A sublattice of the top layer just above B_1 (Fig.1, left). This simplest model accounts for the parabolic dispersion with zero gap at K and K' points of bilayer graphene (Fig.1, right). For the randomness, we consider a bond disorder that is spatially correlated. This is described by a random component, $\delta t(\mathbf{r})$, for the hopping amplitude in each layers as $t(\mathbf{r}) = t + \delta t(\mathbf{r})$, that is gaussian-distributed with a variance σ and is correlated in space with a correlation length η as $\langle \delta t(\mathbf{r}) \delta t(\mathbf{r}') \rangle = \langle \delta t^2 \rangle \exp(-|\mathbf{r} - \mathbf{r}'|^2/4\eta^2)$. It is to be noted that in this tight-binding lattice model the chiral symmetry is exactly preserved even in the presence of disordered components in hopping amplitudes t and γ_1 ,^{7,10} which is due to the bipartite structure of the lattice. Spin degrees of freedom are suppressed for simplicity.

A randomness is expected to be induced in the hopping amplitudes as a consequence of ripples²³ in a monolayer graphene. In the case of bilayer, the disorder should be correlated between the two layers if the two layers have a common ripple. In present paper, however, we also examine the case where the disorder in two layers are uncorrelated to clarify the generality of the topological protection of the Landau levels in bilayer graphene.

The effect of the magnetic field is taken into account by the Peierls substitution $t \rightarrow te^{-2\pi i\theta(\mathbf{r})}$, such that the summation of the phases along a loop is equal to the magnetic flux enclosed by the loop in units of the flux quantum $\phi_0 = (h/e)$. The nearest-neighbor distance of the honeycomb lattice is denoted by a , while the external uniform magnetic flux enclosed by the hexagon of the honeycomb lattice by ϕ .

Zero-mode Landau level — Let us first discuss the robustness of the zero-energy Landau levels. The density of states $\rho(E) = -\langle \text{Im} G_{ii}(E + i\varepsilon)/\pi \rangle_i$ with $G_{ii}(E + i\varepsilon) = \langle i | (E - H + i\varepsilon)^{-1} | i \rangle$ is evaluated by the Green function method.²⁴ Figure 2 displays the density of states for the case where the disorders in the two layers are perfectly

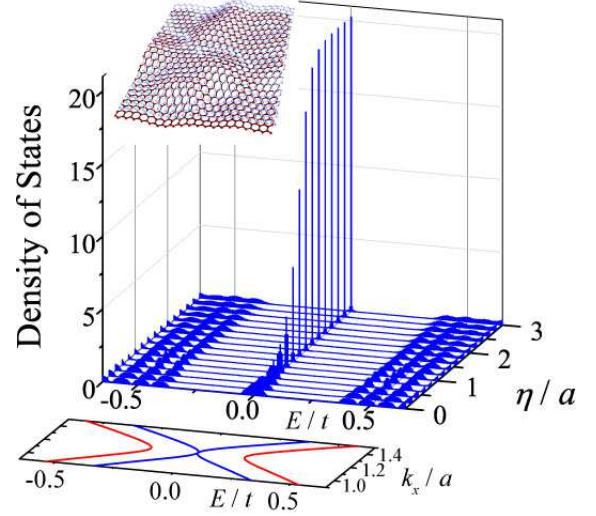


FIG. 2: (Color Online) Density of states of bilayer graphene in a magnetic field plotted for varied correlation length, η , of the bond disorder. The result is for a system with 10^6 sites, a magnetic field $\phi/\phi_0 = 1/50$, the degree of disorder $\sigma/t = 0.115$, inter-layer transfer $\gamma_1/t = 0.2$, and $\varepsilon/t = 0.0006$. Energy dispersion in zero magnetic field around the K point is also shown with the same energy scale. Inset: Schematic figure of correlated ripple.

correlated. We find that the zero energy Landau level becomes anomalously sharp as soon as the spatial correlation length η exceeds a few nearest-neighbor distances a , which is the same behavior as in the case of the monolayer graphene. This means that both of the $n = 0$ and the $n = 1$ Landau levels at zero energy remain delta-function like in the presence of finite-range bond disorder, which confirms the prediction based on the effective Hamiltonian at low energies.¹⁷ We also examine the case where the disorder in two layers is uncorrelated to find that the density of states coincides with those in the correlated case, which reveals an insensitivity to the disorder correlation between two layers (Fig.3).

Electric field effect — In a bilayer graphene we can introduce an energy gap by applying an electric field perpendicular to the graphene sheet (Fig.4, inset).²³ While the electric field obviously breaks the inversion symmetry of the system, we should note that it also breaks the chiral symmetry for the effective Hamiltonian around K and K'. To examine what happens to the robustness of the Landau levels around $E = 0$ in such a case, we evaluate the density of states when the potential difference 2Δ is introduced between the two layers, where the four-fold degenerated zero-energy Landau levels split into four.¹⁶ The present numerical result, displayed in Fig.4, shows that, among the split four Landau levels, the $n = 0$ Landau levels that are located at energies $E = \pm\Delta$ again become anomalously sharp as soon as the disorder is correlated over few lattice constants, while the $n = 1$ Landau levels are broadened by the disorder despite the fact that they are located closer to $E = 0$. An interesting ob-

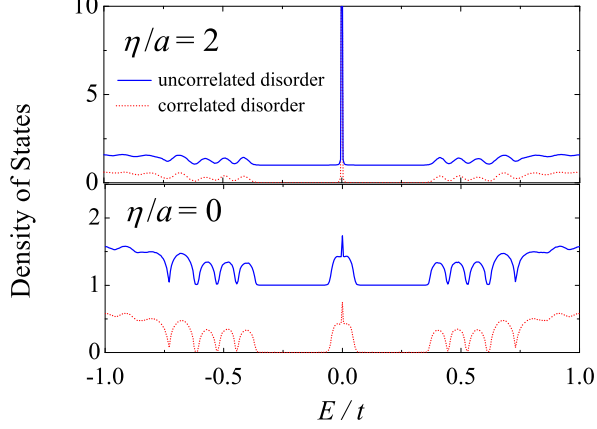


FIG. 3: (Color Online) Density of states of bilayer graphene for the case of correlated disorder *between two layers* (dotted curves) and that for uncorrelated disorder (solid curve) are shown with an offset 1.0 for uncorrelated disorder. The other parameters are the same as in Fig.2.

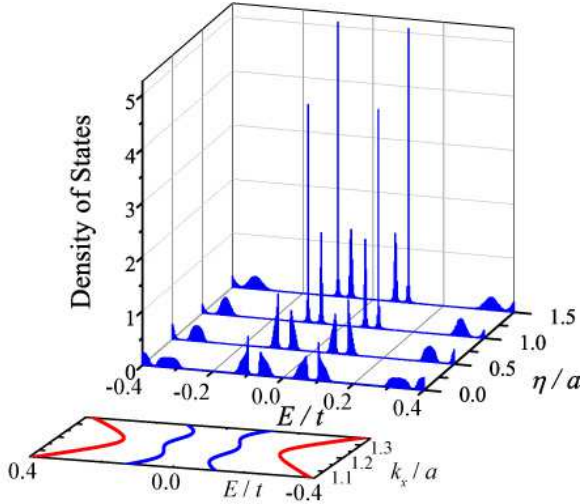


FIG. 4: (Color Online) Density of states of bilayer graphene in the presence of a potential difference $\Delta/t = 0.1$. The other parameters are the same as in Fig. 1. Energy dispersion in zero magnetic field around the K point is also shown in the same energy scale.

servation is that the energies of these anomalously sharp Landau levels can be tuned by the electric field. We can also note that the $n = 1$ Landau levels, while not as sharp as the $n = 0$ Landau levels, are significantly sharper than higher Landau levels. We have also confirmed that the results are insensitive to whether the disorder is correlated between the two layers or not (Fig.5).

Effective theory — The effective Hamiltonian, acting on the envelop functions ($\Psi_{A_2}^K, \Psi_{B_1}^K, \Psi_{A_1}^K, \Psi_{B_2}^K$) at K-point, for bilayer graphene in a perpendicular electric

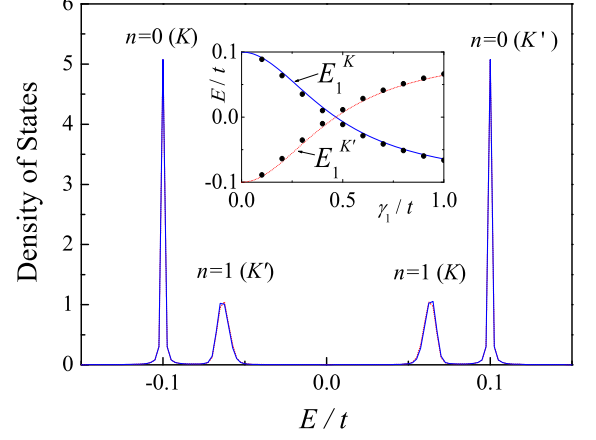


FIG. 5: (Color Online) Four Landau levels split by the electric field around zero energy of bilayer graphene when the disorder correlation length in each layer is $\eta/a = 2$. Here $\Delta/t = 0.1$ and the other parameters are the same as in Fig. 2. The results (solid curve) for the case where the disorder is uncorrelated between two layers is plotted on those (dotted curve) for the case of the same disorder in two layers. Two curves almost coincide, demonstrating clearly the insensitivity to whether the disorder is correlated between the layers or not. A small width of the $n = 0$ levels is an artifact of a finite imaginary energy ε in the Green function. Inset: The energies of the $n = 1$ Landau levels in the presence of disorder are plotted by solid circles as a function of the interlayer coupling γ_1 . The solid(dotted) curve represents the perturbational results (Eq. (1)) for $K(K')$.

field is given by^{16,25,26}

$$H = \begin{pmatrix} \Delta & \gamma_1 & 0 & v_F \pi_2^\dagger \\ \gamma_1 & -\Delta & v_F \pi_1 & 0 \\ 0 & v_F \pi_1^\dagger & -\Delta & 0 \\ v_F \pi_2 & 0 & 0 & \Delta \end{pmatrix},$$

where $\pi_\ell = p_{x\ell} - ip_{y\ell}$ with $\mathbf{p}_\ell = -i\hbar\boldsymbol{\partial} + e\mathbf{A}_\ell$ ($e > 0$), and v_F the Fermi velocity of a monolayer graphene. Here $\ell (= 1, 2)$ labels the two layers, and the gauge field \mathbf{A}_ℓ represents the effective gauge field in each layer, which includes the random gauge field induced by the random hopping as well as the contribution by the external (uniform) magnetic field. The operator π_ℓ satisfies a commutation relation, $[\pi_\ell, \pi_\ell^\dagger] = 2\hbar e B_\ell$, with $B_\ell = (\nabla \times \mathbf{A}_\ell)_z$. Note that the gauge fields \mathbf{A}_1 and \mathbf{A}_2 , and consequently the effective magnetic fields B_1 and B_2 at K point, can be different when the random bonds are different between the two layers.

An important point is that the random component in the gauge field induced by the bond disorder gives rise to effective magnetic fields that have opposite signs between K and K' points.²³ Still, the effective Hamiltonian is chiral-symmetric, since it satisfies $\Gamma H \Gamma = -H$ as long as $\Delta = 0$, where the chiral operator Γ is given, for a

bilayer, in terms of a Pauli matrix σ_z as

$$\Gamma = \begin{pmatrix} \sigma_z & 0 \\ 0 & \sigma_z \end{pmatrix}.$$

The zero modes for the valley K with no electric field ($\Delta = 0$) are, in analogy with the case without disorder,²⁵ given by

$$\Psi_{n=0}^K = \begin{pmatrix} 0 \\ 0 \\ \psi_0^{(1)} \\ 0 \end{pmatrix} \quad \text{and} \quad \Psi_{n=1}^K = \begin{pmatrix} \psi_0^{(2)} \\ 0 \\ -\frac{\gamma_1}{v_F} \psi_1 \\ 0 \end{pmatrix}$$

with $\pi_1 \psi_0^{(1)} = 0$, $\pi_1 \psi_1 = \psi_0^{(2)}$ and $\pi_2 \psi_0^{(2)} = 0$. Note that these zero modes are also eigenstates of the chiral operator Γ .

Following the argument by Aharonov and Casher¹⁴, we adopt the Coulomb gauge $\partial_x^2 A_x + \partial_y^2 A_y = 0$, and express the gauge field as $\mathbf{A} = (-\partial_y \varphi, \partial_x \varphi)$. The operator π is then expressed as $\pi_\ell = -2i\hbar[\partial_{z^*} + 2\pi(\partial_{z^*} \varphi_\ell)/\phi_0]$ with $z \equiv (x + iy)/2$. The solution to $\pi_\ell \psi_0^{(\ell)} = 0$ with $\ell = 1, 2$ is given by $\psi_0^{(\ell)} = f_\ell(z) \exp(-2\pi\varphi_\ell/\phi_0)$, where $f_\ell(z)$ a polynomial in z .¹⁴ In general, the solution ψ_1 takes the form $\psi_1 = f_2(z) \exp(-2\pi\varphi_1/\phi_0) F(z, z^*)$, with $\partial_{z^*} F(z, z^*) = \exp(2\pi(\varphi_1 - \varphi_2)/\phi_0)$. If the bond disorders in two layers are the same ($\varphi_1 = \varphi_2$), the function $F(z, z^*)$ is reduced to z^* .¹⁸ It is straightforward to apply these arguments to the effective Hamiltonian for the valley K',^{16,25,26} which implies that the four-fold degenerated zero-energy Landau levels exist irrespective of presence or absence of the disorder in gauge fields.

When the electric field is switched on ($\Delta \neq 0$), the above chiral symmetry is broken. We can still show, however, that the state $\Psi_{n=0}^K$ remains to be an exact eigenstate of the Hamiltonian with the eigenvalue $\epsilon_0^K = -\Delta$, so that *the broadening due to disorder is absent* as in the case of $\Delta = 0$ is demonstrated. The state $\Psi_{n=1}^K$, on the other hand, is not an exact eigenstate for $\Delta \neq 0$. It is therefore natural to expect that the broadening occurs for the Landau levels corresponding to $\Psi_{n=1}^K$, as is actually seen in our numerical results (Figs. 4 and 5). We can also note that even for such states, the broadening itself is likely to be significantly smaller than those for higher Landau levels, which comes from the anomalous character of the unperturbed Landau level $\Psi_{n=1}^K$ (Fig. 4).

The eigenvalue E_1^K for the state $\Psi_{n=1}^K$ can be estimated, in the absence of disorder, from the perturbation with respect to Δ , which gives

$$E_1^K = \left(1 - \frac{2\gamma_1^2}{2v_F^2 \hbar e B + \gamma_1^2}\right) \Delta, \quad (1)$$

where $B = B_1 = B_2$ denotes the uniform external magnetic field. Relations to the tight-binding parameters

are given by $v_F = (3/2)at/\hbar$ and $\phi = (3\sqrt{3}/2)Ba^2$. The energy E_1^K is then estimated as $E_1^K \simeq 0.7\Delta$ for $\phi = (1/50)\phi_0$ and $\gamma_1/t = 0.2$, which accurately agrees with the present numerical result (Fig.5). The same argument for the effective Hamiltonian at K' point leads to the Landau levels at $E_0^{K'} = -E_0^K = \Delta$ and $E_1^{K'} = -E_1^K \simeq -0.7\Delta$. We also examine the positions of the $n = 1$ Landau levels for various values of the interlayer coupling γ_1 to confirm that their positions are in good agreement with the perturbational result (Eq.(1)) for the range $0 < \gamma_1 < t$ (Fig.5, inset).

The peak heights of these valley-split Landau levels depend on the effective magnetic field for each valley. Since the effective fields induced by ripples in K and K' points have the opposite sign with the same magnitude,²³ the degeneracies of the Landau levels can be different for K and K', although their sum should be a constant.¹⁸ In our numerical results, however, no significant difference in the peak heights for the valley-split Landau levels is seen (Figs.4 and 5). This can be attributed to the fact that the present density of states is an average over the sample. Our sample-size is much larger than the correlation length of bond disorder and the periodic boundary condition is adopted along the strip geometry.⁷ It is therefore expected that the local fluctuation of the magnetic field due to the bond disorder (ripples) is canceled.

Conclusions — We have demonstrated, both numerically and analytically, that the zero-energy Landau levels of bilayer graphene become anomalously sharp when the bond disorder is correlated over a few lattice constants. The anomaly is shown to be insensitive to the disorder correlation between the top and the bottom layers, which suggests a relevance of the chiral symmetry to the present anomaly as in the case of the monolayer graphene. Another new finding is that the anomaly at the $n = 0$ Landau level persists even in the case where the chiral symmetry for each valley is broken by the potential difference between two layers. The splitting of the pair of sharp Landau levels is controlled by the electric field, and their peak heights reflect the effective magnetic field strength at each valley. The anomalous sharpness of these levels found here may help to detect experimentally the local fluctuation of the effective magnetic field arising from ripples as unbalanced peak heights of these Landau levels in the *local* density of states.

Acknowledgments

We wish to thank Yoshiyuki Ono and Takahiro Morimoto for useful discussions and comments. The work was supported in part by Grants-in-Aid for Scientific Research, Nos. 22540336 and 23340112 from JSPS. YH was also supported in part by Grants-in-Aid No.23654128 (JSPS), No. 22014002 (MEXT) and National Science Foundation under Grant No. PHY05-51164.

-
- ¹ K.S. Novoselov et al, Nature **438**, 197 (2005).
 - ² Y. Zhang, Y.W. Tan, H.L. Stormer, and P. Kim, Nature **438**, 201 (2005).
 - ³ P.M. Ostrovsky, I.V. Gornyi, and A.D. Mirlin, Phys. Rev. B **77**, 195430 (2008).
 - ⁴ F. Guinea, B. Horovitz, and P. Le Doussal, Phys. Rev. B **77**, 205421 (2008).
 - ⁵ A.W.W. Ludwig et al, Phys. Rev. B **50**, 7526 (1994).
 - ⁶ Y. Hatsugai, arXiv:1008.4653.
 - ⁷ T. Kawarabayashi, Y. Hatsugai, and H. Aoki, Phys. Rev. Lett. **103**, 156804 (2009); Physica E **42**, 759 (2010).
 - ⁸ T. Kawarabayashi, T. Morimoto, Y. Hatsugai, and H. Aoki, Phys. Rev. B **82**, 195426 (2010).
 - ⁹ A.J.M. Giesbers, U. Zeitler, M.I. Katsnelson, L.A. Ponomarenko, T.M. Mohiuddin, and J.C. Maan, Phys. Rev. Lett. **99**, 206803 (2007).
 - ¹⁰ T. Kawarabayashi, Y. Hatsugai, T. Morimoto, and H. Aoki, Phys. Rev. B **83**, 153414 (2011).
 - ¹¹ S. Katayama, A. Kobayashi, and Y. Suzuura, J. Phys. Soc. Jpn. **75**, 054705 (2006).
 - ¹² M.O. Goerbig, J.-N. Fuchs, G. Montambaux, and F. Piéchon, Phys. Rev. B **78**, 045415 (2008).
 - ¹³ N. Tajima, S. Sugawara, R. Kato, Y. Nishio, and K. Kajita, Phys. Rev. Lett. **102**, 176403 (2009).
 - ¹⁴ Y. Aharonov and A. Casher, Phys. Rev. A **19**, 2461 (1979).
 - ¹⁵ M. Nakahara, *Geometry, Topology, and Physics*, 2nd ed. (Taylor & Francis, 2003).
 - ¹⁶ E. McCann and V.I. Falko, Phys. Rev. Lett. **96**, 086805 (2006).
 - ¹⁷ M.I. Katsnelson and M.F. Prokhorova, Phys. Rev. B **77**, 205424 (2008).
 - ¹⁸ J. Kailasvuori, Europhys. Lett. **87**, 47008 (2009).
 - ¹⁹ R. T. Weitz, M. T. Allen, B. E. Feldman, J. Martin, and A. Yacoby, Science **330**, 812 (2010).
 - ²⁰ J. Martin, B. E. Feldman, R. T. Weitz, M. T. Allen, and A. Yacoby, Phys. Rev. Lett. **105**, 256806 (2010).
 - ²¹ T. Ohta, A. Bostwick, T. Seyller, K. Horn, and E. Rotenberg, Science **313**, 951 (2006).
 - ²² E.V. Castro et al., Phys. Rev. Lett. **99**, 216802 (2007).
 - ²³ A.H. Castro Neto et al, Rev. Mod. Phys. **81**, 109 (2009).
 - ²⁴ L. Schweitzer, B. Kramer, and A. MacKinnon, J. Phys. C **17**, 4111 (1984).
 - ²⁵ M. Koshino, T. Nakanishi, and T. Ando, Phys. Rev. B **82**, 205436 (2010).
 - ²⁶ T. Nakanishi, M. Koshino, and T. Ando, Phys. Rev. B **82**, 125428 (2010).